Published September 24, 2001

JCB Article

Dense core secretory vesicles revealed as a dynamic Ca^{2+} store in neuroendocrine cells with a vesicle-associated membrane protein aequorin chimaera

Kathryn J. Mitchell,[1] Paolo Pinton,[2,3] Aniko Varadi,[1] Carlo Tacchetti,[4] Edward K. Ainscow,[1] Tullio Pozzan,[3] Rosario Rizzuto,[2] and Guy A. Rutter[1]

[1]Departments of Biochemistry, University of Bristol, BS8 1TD Bristol, United Kingdom
[2]Experimental and Diagnostic Medicine Section of General Pathology, University of Ferrara, 44100 Ferrara, Italy
[3]Biomedical Sciences and CNR Center for Study of Biological Membranes, University of Padova, 35121 Padova 17, Italy
[4]Experimental Medicine, University of Genova Medical School, 16132 Genova, Italy

The role of dense core secretory vesicles in the control of cytosolic-free Ca^{2+} concentrations ($[Ca^{2+}]_c$) in neuronal and neuroendocrine cells is enigmatic. By constructing a vesicle-associated membrane protein 2–synaptobrevin.aequorin chimera, we show that in clonal pancreatic islet β-cells: (a) increases in $[Ca^{2+}]_c$ cause a prompt increase in intravesicular-free Ca^{2+} concentration ($[Ca^{2+}]_{SV}$), which is mediated by a P-type Ca^{2+}-ATPase distinct from the sarco(endo) plasmic reticulum Ca^{2+}-ATPase, but which may be related to the PMR1/ATP2C1 family of Ca^{2+} pumps; (b) steady state Ca^{2+} concentrations are 3–5-fold lower in secretory vesicles than in the endoplasmic reticulum (ER) or Golgi apparatus, suggesting the existence of tightly bound and more rapidly exchanging pools of Ca^{2+}; (c) inositol (1,4,5) trisphosphate has no impact on $[Ca^{2+}]_{SV}$ in intact or permeabilized cells; and (d) ryanodine receptor (RyR) activation with caffeine or 4-chloro-3-ethylphenol in intact cells, or cyclic ADPribose in permeabilized cells, causes a dramatic fall in $[Ca^{2+}]_{SV}$. Thus, secretory vesicles represent a dynamic Ca^{2+} store in neuroendocrine cells, whose characteristics are in part distinct from the ER/Golgi apparatus. The presence of RyRs on secretory vesicles suggests that local Ca^{2+}-induced Ca^{2+} release from vesicles docked at the plasma membrane could participate in triggering exocytosis.

Introduction

In most mammalian cells, the ER (Streb et al., 1984; Rizzuto et al., 1993; Brini et al., 1993) and Golgi complex (Pinton et al., 1998) are believed to represent the major mobilizable intracellular Ca^{2+} stores (Rutter et al., 1998). Uptake of Ca^{2+} into these stores is mediated largely by sarco(endo)plasmic reticulum Ca^{2+}–ATPases (SERCAs)* (Moller et al., 1996) and helps to maintain resting cytosolic Ca^{2+} concentrations ($[Ca^{2+}]_c$) at levels ($\sim 10^{-7}$ M) some four orders of magnitude lower than in the extracellular space ($\sim 10^{-3}$ M). Release of Ca^{2+} from the ER and Golgi complex is provoked by hormones and other agonists which generate inositol 1,4,5 trisphosphate (IP_3) (Berridge, 1993) to open intracellular receptors (Mikoshiba, 1997). In certain cell types, such as skeletal muscle, these stores are also accessed by "Ca^{2+}-induced Ca^{2+} release", via receptors for the insecticide, ryanodine (Lai et al., 1988; Takeshima et al., 1989).

Secretory vesicles of both the dense core (Hellman et al., 1976; Hutton et al., 1983) and small synaptic types (Andrews and Reese, 1986) possess a substantial proportion of the total Ca^{2+} in cells specialized for peptide secretion. However, despite many studies, the role of secretory vesicles as Ca^{2+} buffers or stores remains controversial (Pozzan et al., 1994; Rutter et al., 1998; Yoo, 2000).

Mobilization of dense core vesicle Ca^{2+} by IP_3 was originally suggested as a possibility in chromaffin cells (Yoo and Albanesi, 1990). Later data suggested that IP_3 receptors may be present on the vesicle membrane in insulin-secreting cells (Blondel et al., 1994), though subsequent experiments

Address correspondence to Guy Rutter, Department of Biochemistry, University of Bristol, BS8 1TD Bristol, UK. Tel.: (44) 117-954-6401. Fax: (44) 117-928-8274. E-mail: g.a.rutter@bris.ac.uk

*Abbreviations used in this paper: cADPr, cyclic ADP ribose; CPA, cyclopiazonic acid; DHPG, dihydroxyphenylglycine; GFP, green fluorescent protein; HA, hemagglutinin; IB, intracellular buffer; IP_3, inositol 1,4,5 trisphosphate; KRB, Krebs-Ringer bicarbonate buffer; RyR, ryanodine receptor; 4-CEP, 4-chloro-3-ethylphenol; SERCA, sarco(endo)plasmic reticulum Ca^{2+}–ATPase; VAMP, vesicle-associated membrane protein.

Key words: calcium; secretory vesicle; insulin; ryanodine receptor; aequorin

Published September 24, 2001

showed the antibody used cross-reacted with insulin (Ravazzola et al., 1996). IP_3, as well as the receptor (RyR) agonist cyclic ADP ribose (cADPr) (Galione, 1994) have been reported to release Ca^{2+} from individual acinar cell zymogen granules (Gerasimenko et al., 1996), although contamination of these preparations (e.g., with ER or Golgi apparatus–derived vesicles) is a potential problem (Yule et al., 1997). Finally, evidence for the direct participation of secretory granules in the control of cytoplasmic Ca^{2+} concentration was recently provided in intact goblet cells (Nguyen et al., 1998).

At present, the molecular mechanisms responsible for Ca^{2+} uptake into secretory vesicles are also a matter of controversy. At high Ca^{2+} concentrations (>50 μM), uptake into dense core vesicles in permeabilized hypophysial cells (Troadec et al., 1998; Thirion et al., 1999) and into isolated chromaffin cell granules (Krieger-Brauer and Gratzl, 1982) can occur via Na^+/Ca^{2+} exchange, while synaptic vesicles also accumulate Ca^{2+} via a Ca^{2+}-H^+ antiport system (Goncalves et al., 1998). However, the pump/exchange mechanisms active at physiological $[Ca^{2+}]_c$ are uncertain.

To examine the pathways by which Ca^{2+} crosses the limiting membrane of the dense core secretory vesicle of living islet β-cells, we have developed a new approach to monitor the free Ca^{2+} concentration within the secretory vesicle matrix ($[Ca^{2+}]_{SV}$) using recombinant targeted aequorin (Rizzuto et al., 1995). Cloned from the jellyfish *Aequorea victoria* (Inouye et al., 1985), aequorin is a calcium-sensitive bioluminescent protein (Cobbold and Rink, 1987), previously used to measure free Ca^{2+} concentrations in a variety of subcellular organelles (Rutter et al., 1998). Importantly, aequorin activity is less severely inhibited at low pH values (<6.5; Blinks, 1989) than Ca^{2+} probes based on green fluorescent protein (GFP) (Miyawaki et al., 1997; Baird et al., 1999; Emmanouilidou et al., 1999). If appropriately targeted, this probe should allow Ca^{2+} concentrations to be measured in the acidic environment of the secretory granule interior (Orci et al., 1985).

Vesicle-associated membrane protein (VAMP)2/synaptobrevin (Sudhof et al., 1989) is a vesicle-specific SNARE with a single transmembrane-spanning region. Expression of chimaeric cDNA encoding a fusion protein between VAMP2 and aequorin (VAMP.Aq) has therefore allowed the intravesicular-free Ca^{2+} concentration to be monitored dynamically in live MIN6 β-cells. With this approach, we show that Ca^{2+} is actively pumped into dense core vesicles when $[Ca^{2+}]_c$ increases, and may be released via RyR, but not IP_3, receptors. This release may be important at sites of high intracellular Ca^{2+}, including sites of exocytosis at the plasma membrane.

Results

Subcellular targeting of recombinant VAMP.aequorin

Chimeric cDNA encoding hemagglutinin (HA)1-tagged aequorin, fused to VAMP2 (Sudhof et al., 1989), was generated as shown in Fig. 1 A.

Immunocytochemical analysis of MIN6 cells transfected with VAMP.Aq cDNA revealed close overlap with insulin staining (Fig. 1 B). Explored at a higher resolution by immunoelectron microscopy (Fig. 1 C), VAMP.Aq immunoreactivity was highly enriched in 61 of 148 (41.2%; $n = 11$ cells) vesicles

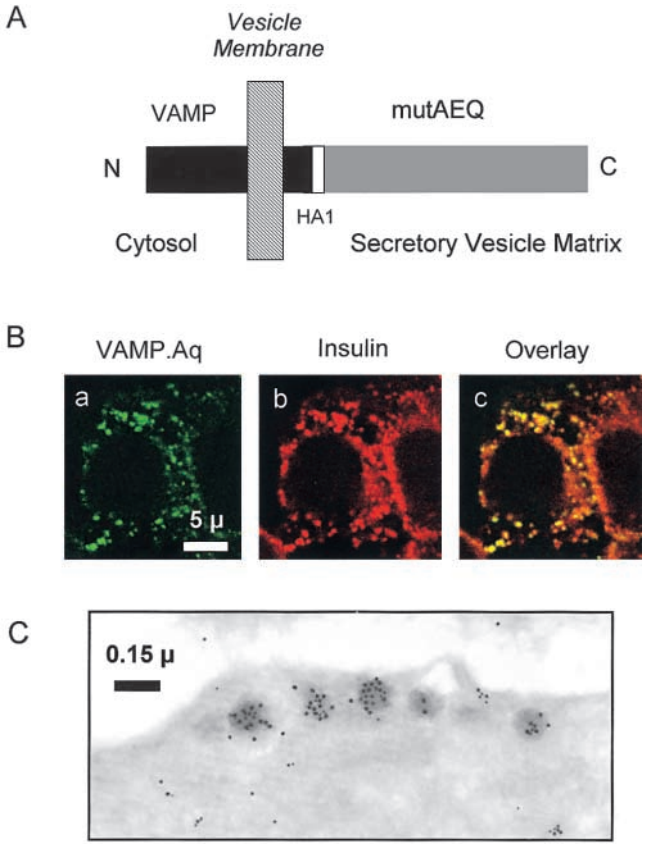

Figure 1. **Localization of VAMP.Aq.** (A) Schematic map of VAMP.Aq. VAMP2 and aequorin cDNAs were fused via an HA1 epitope tag linker (Materials and methods) in order to localize mutated aequorin to the secretory vesicle lumen. (B) Confocal immunolocalization of VAMP.Aq. MIN6 cells were transfected with VAMP.Aq and stained with (a) mouse anti-HA1 monoclonal antibody (1:200) and (b) guinea pig antiinsulin antibody (1:150). (c) Extent of colocalization. (C) Immunoelectron microscopic localization of insulin (15-nm gold) or VAMP.Aq (anti-HA tag, 10-nm gold). Morphometric analysis of separate sections from 10 singly labeled cells revealed the following distribution of anti-HA gold particles: dense core vesicles, 36; ER, 2; Golgi apparatus, 0; plasma membrane, 16; endosomes, 19.

colabeled for insulin (Fig. 1 C). Analyzed by single labeling for VAMP.Aq, staining of the ER, Golgi apparatus, and small synaptic-like microvesicles (Reetz et al., 1991) was very low, while reactivity was also present on the plasma membrane and in endosomes (see the legend to Fig. 1 and Discussion).

Reconstitution and calibration of secretory vesicle and ER-targeted aequorins

Given the high total Ca^{2+} content of secretory vesicles (Hutton et al., 1983), we used the approach adopted previously to measure Ca^{2+} in the ER lumen (Montero et al., 1995). Apoaequorin was reconstituted at a low free Ca^{2+} concentration (Montero et al., 1995), achieved by depleting cells of Ca^{2+} (Materials and methods). Depletion of vesicle Ca^{2+} had no marked effect on glucose or K^+-stimulated insulin secretion, or on vesicle motility (Pouli et al., 1998b; Tsuboi et al., 2000; unpublished data).

To determine the response of the expressed aequorins to Ca^{2+} in situ, permeabilized cells were incubated at buffered

Published September 24, 2001

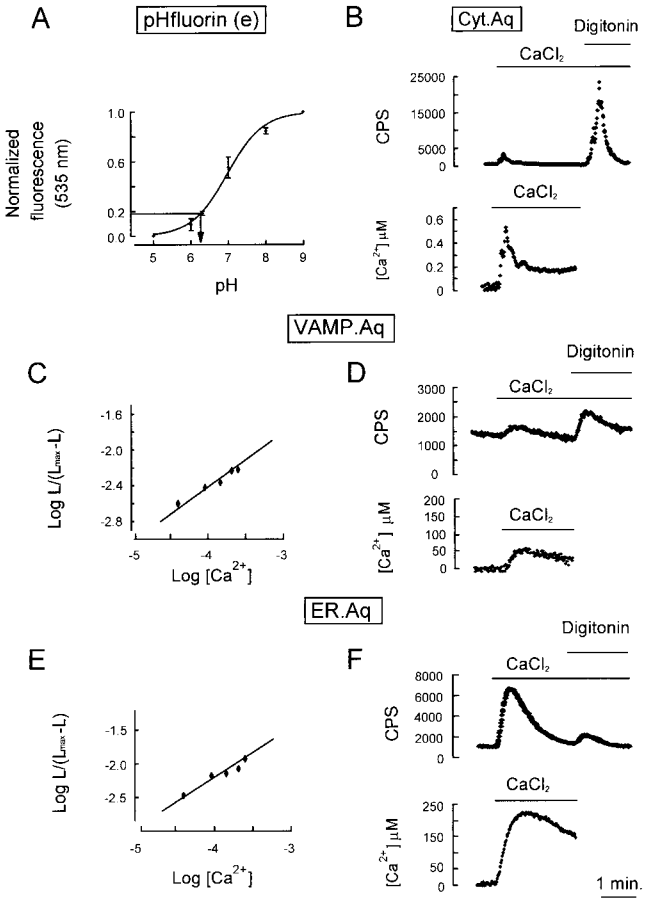

Figure 2. **Measurement of intravesicular pH (A) and Ca^{2+} with cytosolic aequorin (B), VAMP.Aq (C and D), and ER.Aq (E and F).** (A) Confocal images were acquired from cells transfected with pH.fluorin(e) (Miesenbock et al., 1998), maintained initially in KRB, pH 7.4, before digitonin-permeabilization and exchange into IB at the specified pH values, and buffered with morpholinosulphonic acid, Hepes, or TRIS (10 mM), plus 10 µM ionomycin, 10 µM monensin, and 1 µM FCCP. Normalized fluorescence ratios before permeabilization were in the range of 0.16–0.18 (arrow); data were fitted using the Graph Pad Prism™. (C and E) After Ca^{2+} depletion and aequorin reconstitution, transfected cells were permeabilized with digitonin and perifused in the presence of ionomycin, monensin, and CPA (10 µM each) with N-(2-hydroxyethyl)ethylene diamine triacetate (HEDTA)-buffered Ca^{2+} solutions at 0.5 mM calculated free Mg^{2+}. Cells expressing either (B) cytosolic aequorin, (D) VAMP.Aq, or (F) ER.Aq were perifused with KRB, supplemented with 1 mM EGTA (KRB/EGTA) and, where indicated, EGTA was replaced with 1.5 mM $CaCl_2$. Cells were finally lysed in Ca^{2+}-rich hypotonic medium (10 mM $CaCl_2$, 0.1 mM digitonin) for calibration (see Materials and methods and Results). The background count rate (~1,200 cps; D and F) was identical during perifusion of untransfected cells and is due to autooxidation of coelenterazine *n*.

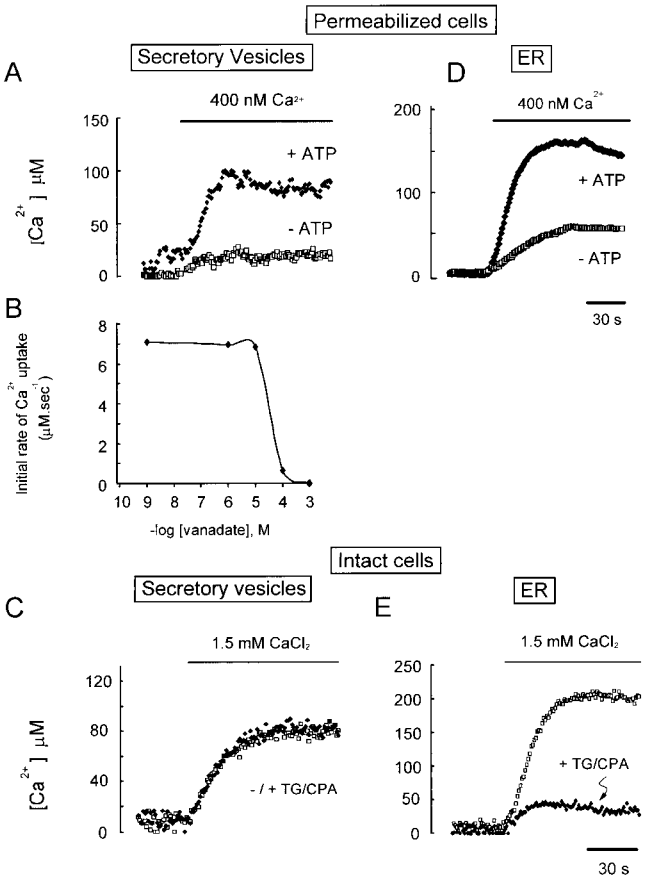

Figure 3. **Ca^{2+} uptake into secretory vesicles (A–C) or ER (D and E).** After Ca^{2+} depletion and aequorin reconstitution, cells were permeabilized with 20 µM digitonin in IB; (A and D; see Materials and methods). Cells were perifused initially at $<10^{-9}$ M free [Ca^{2+}] (buffered with 0.2 mM EGTA, 1 mM HEDTA; free [Mg^{2+}] = 0.5 mM) and then at 400 nM free [Ca^{2+}], as indicated. Where present (closed symbols) ATP was 1 mM. Note that accumulation of Ca^{2+} at zero ATP is likely to be due to synthesis of small amounts of ATP by mitochondria. (B) Dose–response for the inhibition of vesicular [Ca^{2+}] increases by orthovanadate. Cells expressing VAMP.Aq were permeabilized and perifused at 400 nM Ca^{2+} in the presence of 1 mM ATP, plus the indicated concentrations of $NaVO_4$. The initial rates of $[Ca^{2+}]_{SV}$ increase upon the stepped increase in perifusate-free [Ca^{2+}] from <1 to 400 nM were calculated by fitting time course data to a simple first order rate equation by nonlinear regression analysis (Microsoft Excel™). (C and E) After Ca^{2+} depletion and aequorin reconstitution, Ca^{2+} uptake into intact cells was initiated by replacing KRB containing 1 mM EGTA with EGTA-free KRB at 1.5 mM $CaCl_2$, as indicated. Closed symbols, cells were incubated with thapsigargin (TG; 1 µM) during the final 10 min of reconstitution, and the perifusion medium was supplemented with CPA (10 µM). Data are representative of three separate experiments in each case.

Ca^{2+} concentrations in the presence of ionomycin and monensin (Fig. 2, C and E). The sensitivity to Ca^{2+} (at pH 7.0) of the VAMP.Aq chimaera was similar to that reported previously for mutant ($D^{119}A$) aequorin (Montero et al., 1995). Intravesicular pH in intact cells was determined using a fusion construct between VAMP2 and a mutated, pH-sensitive GFP (pH.fluorin(e); Miesenbock et al., 1998), and gave a pH value of 6.3 ± 0.02 (n = 85 cells; Fig. 2 A). Confirming that this low intravesicular pH was unlikely to significantly affect VAMP.Aq, near identical calibration data were obtained at pH 5.7 (unpublished data). Therefore, we used the constants obtained in vitro (Montero et al., 1995) to calculate [Ca^{2+}] from the fractional rate of aequorin consumption (F) according to: $[Ca^{2+}] = 1.44\sqrt{10^{(LOG[F]-3.4)}}$ (Rutter et al., 1993).

Dynamic measurement of secretory vesicle and ER Ca^{2+} concentrations

To monitor uptake of Ca^{2+} into vesicles in living cells, we provoked rapid Ca^{2+} influx into cells through store-operated channels (Parekh and Penner, 1997). During reintroduction

Table I. **Kinetic paramers for Ca^{2+} uptake into the ER versus secretory vesicles**

	Steady state $[Ca^{2+}] \pm$ SE	$t_{1/2} \pm$ SE	$K_{initial}$	*n*
	μM	*s*	*μM/s*	
ER	249 ± 12.9	5.7 ± 0.2	29.8 ± 0.8	3
+Thap	71 ± 12.3	6.1 ± 1.3	9.2 ± 2.7[a]	3
Vesicles	51 ± 7.5	4.2 ± 0.1	7.1 ± 1.1	5
+Thap	40 ± 4.4	3.9 ± 0.6	7.4 ± 0.5	3

Kinetic values were calculated by fitting time course data (Fig. 3) to a simple first order exponential curve by nonlinear least squares regression (Microsoft Excel™).
[a]$P < 1\%$.

of $CaCl_2$ to cells previously perifused in EGTA, $[Ca^{2+}]_c$ approached 500 nM, then fell back to 150–200 nM (Fig. 2 B). By contrast, steady state free $[Ca^{2+}]$ in the secretory vesicle matrix was 30–90 μM (51; 7.5 μM; $n = 5$ separate cultures; Fig. 2 D), whereas free $[Ca^{2+}]$ in the ER lumen was fivefold higher (249; 12.9 μM; $n = 3$ preparations; Fig. 2 F).

Pathways of Ca^{2+} uptake into dense core secretory vesicles

Both the rate and extent of the $[Ca^{2+}]$ increases in the secretory vesicles and the ER were strongly dependent on the presence of added ATP in permeabilized cells (Fig. 3, A and D). The increase in $[Ca^{2+}]_{SV}$ upon reintroduction of Ca^{2+} ions was completely inhibited by the P-type Ca^{2+} pump inhibitor, orthovanadatate, at >100 μM (Fig. 3 B), but was insensitive to 10 μM orthovanadatate, a concentration which strongly inhibits the plasma membrane Ca^{2+}-ATPase (Carafoli, 1991). Preincubation with the specific SERCA inhibitor, thapsigargin (Thastrup, 1990), and perifusion with cyclopiazonic acid (CPA) (Mason et al., 1991) had no effect on the changes in $[Ca^{2+}]_{SV}$ (Fig. 3 C and Table I), but markedly (>85%) inhibited ER $[Ca^{2+}]$ increases (Fig. 3 E).

Arguing against vesicular Ca^{2+} uptake via Ca^{2+}/H^+ exchange, monensin, an Na^+/H^+ exchanger, had no effect on $[Ca^{2+}]_{SV}$ increases in permeabilized cells (Fig. 4 A). Similarly, ionomycin (a Ca^{2+}/H^+ exchanger) decreased $[Ca^{2+}]_{SV}$ marginally (~20%; Fig. 4 B), which is consistent with the inability of this ionophore to bind to and transport Ca^{2+} against a prevailing H^+ gradient, but caused a rapid and complete decline in $[Ca^{2+}]_{SV}$ in the additional presence of monensin (Fig. 4 B). Neither the vacuolar H^+-ATPase inhibitor, bafilomycin (Fig. 4, C and D), nor the protonophore carbonyl cyanide-p-trifluoromethoxyphenylhydrazone (FCCP), had any effect on vesicular Ca^{2+} uptake (Fig. 4 E).

$[Ca^{2+}]_{SV}$ increases were also completely unaffected by raising $[Na^+]$ from 0, 2, or 140 mM (Fig. 4 F), and by simultaneous blockade of Na^+/Ca^{2+} exchange and Ca^{2+}/H^+ exchange (zero Na^+, 300 nM bafilomycin; unpublished data).

Effects of IP_3 on $[Ca^{2+}]_{SV}$ and $[Ca^{2+}]_{ER}$

To achieve large changes in intracellular IP_3 levels, we coexpressed the metabotropic glutamate receptor, mGluR5, with VAMP.Aq or ER.Aq. Stimulation of mGluR5-transfected cells with the specific agonist, (S)-3,5-dihydroxyphenylglycine (DHPG) (Thomas et al., 2000) caused a significant de-

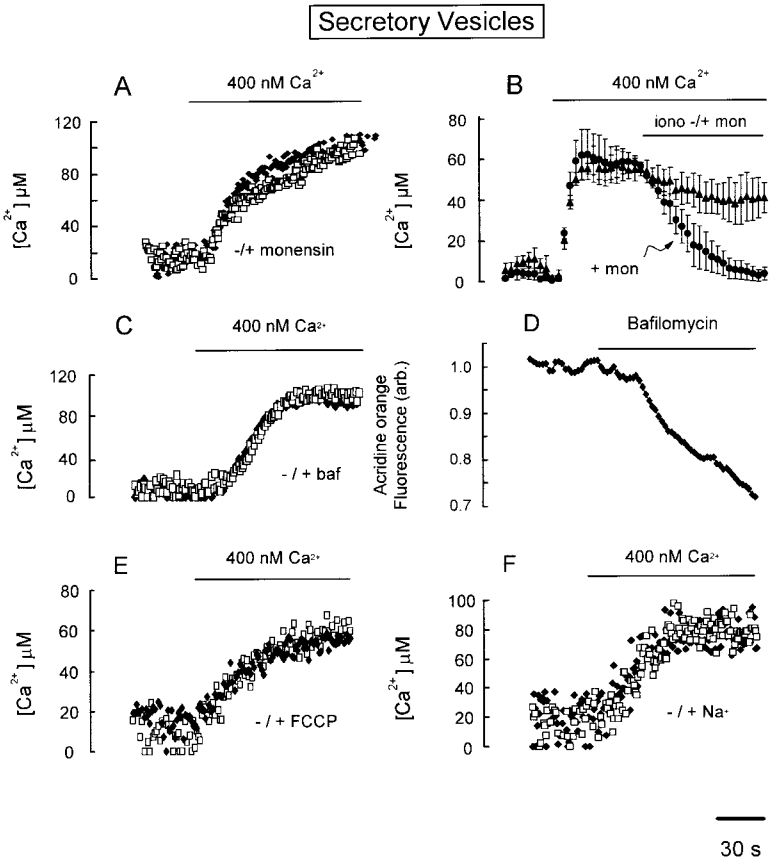

Figure 4. **Effects of collapse of H^+ and Na^+ gradients on vesicular Ca^{2+} accumulation in permeabilized cells.** Cells were Ca^{2+} depleted and aequorin reconstituted with coelenterazine *n* before digitonin permeabilization. Cells were perifused in IB (Materials and methods) and free $[Ca^{2+}]$ was increased from <1 to 400 nM as indicated, either in the absence (A, C, E, and F, open symbols) or in the presence of the additions (closed symbols) as follows: A, 10 μM monensin; B, when indicated, 10 μM ionomycin (triangles), or ionomycin plus 10 μM monensin (circles); C, 300 nM bafilomycin; E, 1 μM carbonyl cyanide-p-trifluoromethoxyphenylhydrazone (FCCP); F, 140 mM NaCl. Trace (D) shows the effect of bafilomycin on vesicular acridine orange fluorescence in 10 individual cells imaged simultaneously (Materials and methods). Data are representative of at least three separate experiments or are the means ± SEM of three (B).

Published September 24, 2001

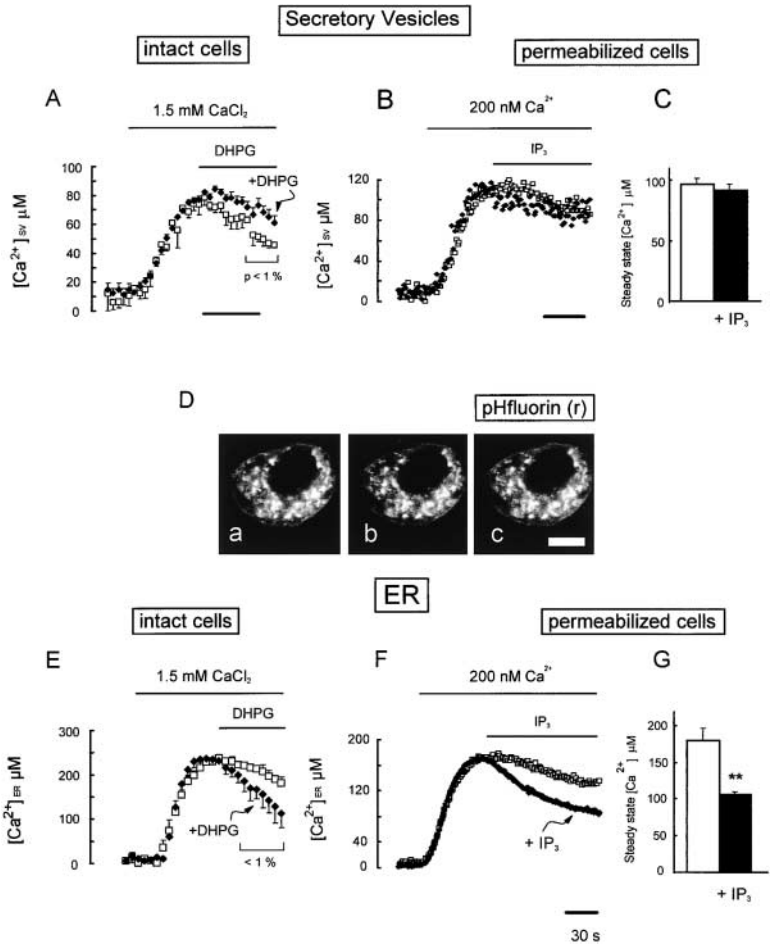

Figure 5. **Effect of IP_3 on $[Ca^{2+}]_{SV}$ and $[Ca^{2+}]_{ER}$ in intact (A and E) and permeabilized (B, C, F, and G) cells.** MIN6 cells were cotransfected with (A) VAMP.Aq or (E) ER.Aq plus a plasmid bearing mGluR5 cDNA. After the depletion of intracellular Ca^{2+} stores and aequorin reconstitution, cells were perifused in KRB, which initially contained 1 mM EGTA. Where indicated, EGTA was replaced with 1.5 mM $CaCl_2$. After the achievement of steady state $[Ca^{2+}]$, cells were challenged with the mGluR5 receptor agonist DHPG (30 μM) as indicated. Data are means of five independent experiments. (B, C, F, and G) Cells transfected with plasmids encoding VAMP.Aq (B and C) or ER.Aq (F and G) were Ca^{2+} depleted and aequorin was reconstituted before permeabilization and perifusion in IB buffer which initially contained 0.1 mM EGTA (free $[Ca^{2+}] < 1$ nM). HEDTA and $CaCl_2$ were added to give a calculated free $[Ca^{2+}]$ of 200 nM, as indicated. After the achievement of steady state $[Ca^{2+}]_{SV}$ or $[Ca^{2+}]_{ER}$, IP_3 (5 μM) was introduced (filled symbols) as shown (B and F). Mean steady state $[Ca^{2+}]_{SV}$ and $[Ca^{2+}]_{ER}$ in three separate experiments in the presence or absence of IP_3 are shown in C and G, respectively. Double asterisk indicates $P < 1\%$ for the effect of IP_3 on $[Ca^{2+}]_{ER}$. D shows cells cotransfected with VAMP.GFP (pH.fluorin(r); Miesenbock et al., 1998) and mGluR5 cDNAs and depleted of Ca^{2+}, as in A. Localization of vesicles (a) after 1 h of Ca^{2+}-depletion, (b) 120 s after readdition of $CaCl_2$, and (c) 60 s after DHPG addition.

crease in $[Ca^{2+}]_{ER}$ (Fig. 5 E), but an increase in $[Ca^{2+}]_{SV}$ (Fig. 5 A). DHPG had no significant effect on the distribution of vesicles (imaged after expression of VAMP.GFP/pHfluorin (r); Fig. 5 D), indicating that enhanced exocytosis and exposure of the VAMP.Aq to the extracellular medium was unlikely to contribute to the observed increases in $[Ca^{2+}]_{SV}$ (Fig. 5 A, and see Discussion).

Similarly, in permeabilized cells, IP_3 had no effect on $[Ca^{2+}]_{SV}$ (Fig. 5, B and C), while causing a large decrease in $[Ca^{2+}]_{ER}$ (Fig. 5, F and G).

RyR activation decreases $[Ca^{2+}]_{SV}$ and $[Ca^{2+}]_{ER}$

The RyR agonists caffeine or 4-chloro-3-ethylphenol (4-CEP) (Zorzato et al., 1993) provoked rapid decreases in $[Ca^{2+}]_{SV}$ and $[Ca^{2+}]_{ER}$ (Fig. 6, A and C) in intact cells. Similarly, cADPr (Galione, 1994) caused clear decreases in both parameters in permeabilized cells (Fig. 6, B and D), and the effects of cADPr were strongly potentiated by palmitoyl CoA (Fig. 6, B and D), a coagonist of RyRs (Chini and Dousa, 1996).

4-CEP mobilizes Ca^{2+} from an acidic, CPA-insensitive store in fura-2–loaded MIN6 cells

The above results suggested that activation of RyR on vesicles should cause an increase in cytoplasmic $[Ca^{2+}]_c$, even after the depletion of the ER Ca^{2+} pool. Added to fura-2–loaded MIN6 cells, 4-CEP caused a substantial increase in $[Ca^{2+}]_c$ in the absence of external Ca^{2+} (Fig. 7 A). This $[Ca^{2+}]_c$ increase was partly retained after depletion of SERCA-dependent stores, giving a peak $[Ca^{2+}]_c$ increase of 30–40% of that in control cells (Fig. 7 B versus A). The $[Ca^{2+}]_c$ increase elicited by 4-CEP was also partially retained after treatment of cells with ionomycin (Fig. 7 C), but completely abolished after treatment with ionomycin plus monensin, to deplete acidic Ca^{2+} stores (Fig. 7 D). Demonstrating that the effects of 4-CEP on $[Ca^{2+}]_{SV}$ were likely mediated by RyR, immunoreactivity to these channels was revealed on vesicle membranes by direct immunoelectron microscopy (Fig. 7 E).

Effects of nutrient secretagogues on $[Ca^{2+}]_{ER}$ and $[Ca^{2+}]_{SV}$

Exposure of islet β- or MIN6 cells to glucose or other nutrients causes an increase in intracellular-free [ATP] (Kennedy et al., 1999) closure of ATP-sensitive K^+ (K_{ATP}) channels (Bryan and AguilarBryan, 1997) and Ca^{2+} entry via voltage-sensitive (L-type) Ca^{2+} channels (Safayhi et al., 1997).

High (20 mM) glucose, or a combination of nutrient secretagogues (Ashcroft and Ashcroft, 1992), caused a large increase in steady state $[Ca^{2+}]$ both in the ER and in vesicles (Fig. 8, A and C), with no significant change in vesicular distribution (Fig. 8 B), which is consistent with the increases in $[Ca^{2+}]_c$ seen under these conditions (Grapengiesser et al., 1988).

Published September 24, 2001

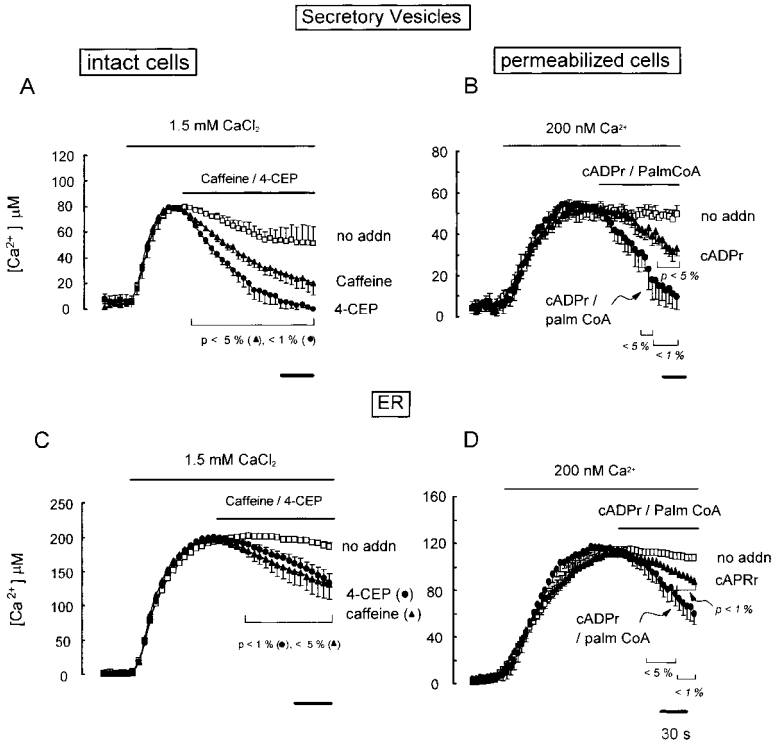

Figure 6. **Effect of RyR agonists on secretory vesicle and ER Ca^{2+} concentrations.** Cells were transfected (A and C) or infected with adenoviruses (B and D) encoding either VAMP.Aq (A and B) or ER.Aq (C and D), then perifused in KRB containing 1 mM EGTA (A and C) or digitonin permeabilized and perifused with IB which initially contained 0.1 mM EGTA (B and D). Replacement of EGTA with 1.5 mM $CaCl_2$ (intact cells, A and C), or an increase in perifusate-free $[Ca^{2+}]$ to 200 nM (permeabilized cells, B and D), as indicated. Other additions were: caffeine, 10 mM; 4-CEP, 500 μM; cADPr, 5 μM; palmitoyl CoA, 50 μM.

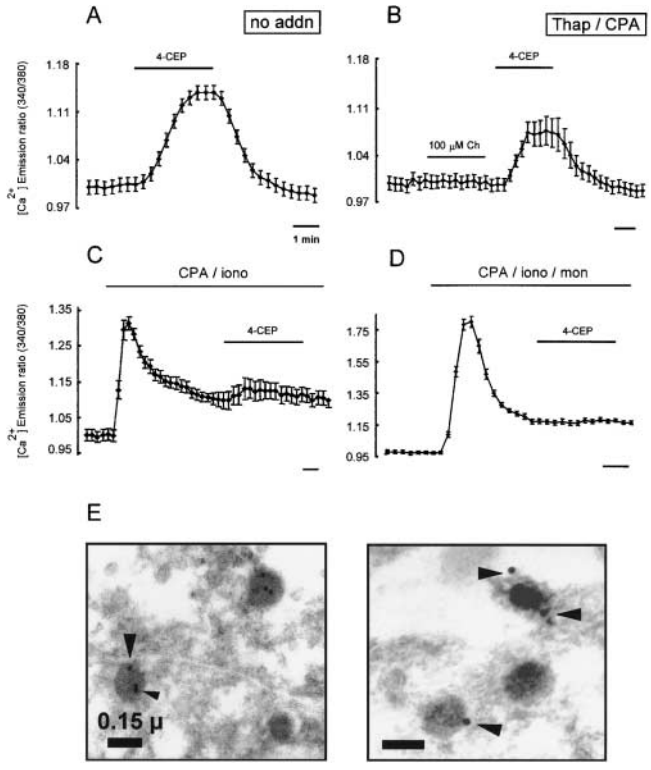

Figure 7. **Effect of caffeine and 4-CEP on cytosolic $[Ca^{2+}]$.** (A–D) Cells were loaded with fura-2 and imaged as described (Materials and methods). Where indicated (B–D), cells were preincubated with 1 μM thapsigargin in Ca^{2+}-free KRB (supplemented with 1 mM EGTA for 10 min) and then subsequently perifused in Ca^{2+}-free medium, initially in the absence of thapsigargin or other additions. Trace (A) shows the effect of 500 μM 4-CEP, added as indicated, on $[Ca^{2+}]_c$ in cells untreated with thapsigargin, and (B) the effect of the drug on cells treated with thapsigargin and subsequently perifused in the presence of 10 μM CPA. Note the abolition of the response to carbachol, which caused a large increase in $[Ca^{2+}]_c$ in untreated cells (unpublished data). In C, CPA and ionomycin (10 μM each) were added as indicated. Panel D was as C, but with the further addition of monensin (mon, 10 μM) to the perifusate. Data are the means (± SEM) on observations on a total of (A) 58, (B) 35, (C) 28, and (D) 40 single cells, imaged in 3–5 separate experiments. (E) Immunoelectron microscopic localization of RyR (arrows) on dense core vesicles.

Discussion

Aequorin as a reporter of secretory vesicle–free Ca^{2+} concentration

We show here that aequorin can be targeted to the lumen of dense core secretory vesicles in living cells, with no incorporation into the ER, Golgi, or trans-Golgi network using the cell's own protein-sorting machinery (Fig. 1). However, a proportion of VAMP.Aq was also present on the plasma membrane and endosomes (Fig. 1 C). Since our recordings were made at either high (1.5 mM, intact cells) or low (400 nM, permeabilized cells) external Ca^{2+} concentrations, the plasma membrane–located photoprotein should be either rapidly exhausted, or inactive, respectively. In any case, it would appear that plasma membrane–targeted aequorin is not reconstituted, since we would have expected to see a "spike" of luminescence upon readdition of high Ca^{2+} concentrations to intact cells (e.g., Fig. 3 C). None was seen, suggesting that the mistargeted protein may be inactivated by unknown mechanisms during recycling between the plasma membrane and endosomes.

Similarly, endosomal aequorin is likely to be inactive under our conditions, since (a) the total endosomal Ca^{2+} content is low in neuroendocrine cells (Pezzati et al., 1997) and (b) free $[Ca^{2+}]$ is particularly low (~3.0 μM) in acidic endosomes (Gerasimenko et al., 1998); active VAMP.Aq was lo-

Published September 24, 2001

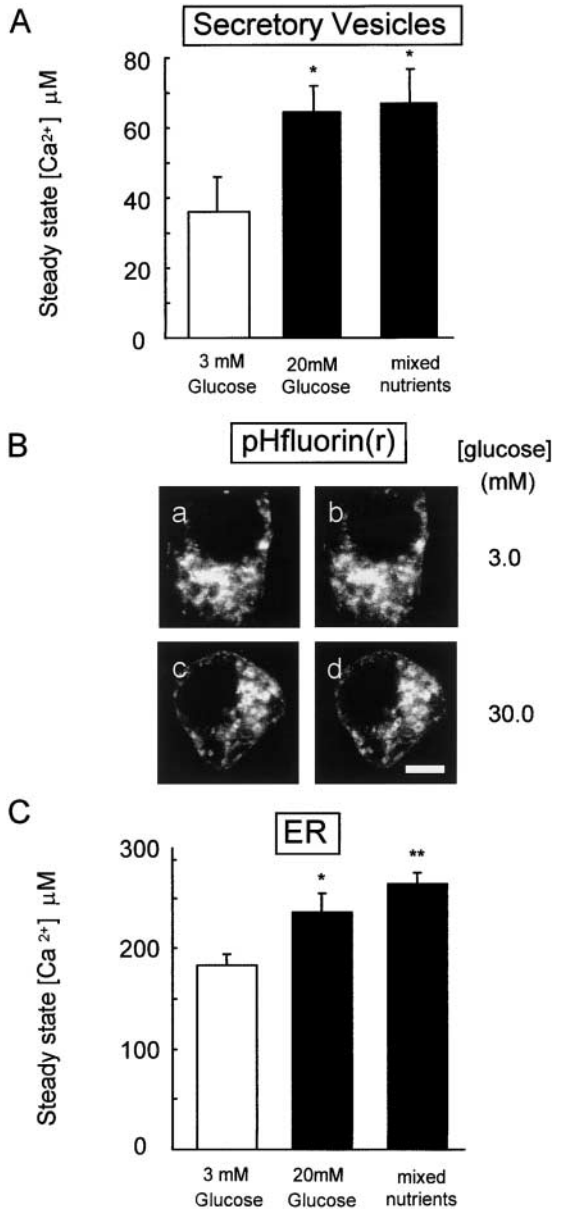

Figure 8. **Effect of nutrient secretagogues on steady state [Ca^{2+}] in secretory vesicles and the ER.** Ca^{2+} depletion, and aequorin reconstitution, were carried out as described in Fig. 3 before exposure of cells expressing VAMP.Aq (A) or ER.Aq (C) to the concentrations of nutrients shown for 2 min in complete KRB medium containing 1.5 mM $CaCl_2$. Mixed nutrients, 20 mM glucose, 10 mM glutamine, 10 mM leucine. In all cases, cells were preperifused for 5 min and maintained in the presence of 1 mM 3-isobutyl-1-methylxanthine (IBMX). Asterisk indicates $P < 5\%$; double asterisk indicates $P < 1\%$ for the effect of 20 mM glucose or mixed nutrients, respectively. In B, cells expressing VAMP.GFP (pH.fluorin(e)) were Ca^{2+} depleted as in A, before (a and c) or after (b and d) reintroduction of $CaCl_2$ in the presence of 3 mM (a and b) or 30 mM (c and d) glucose. Bar, 5 μm.

cated exclusively in an acidic compartment (Fig. 4 B). Simulation of the contribution of endosomal VAMP.Aq reveals that our measurements may slightly underestimate $[Ca^{2+}]_{SV}$ (by <10%; unpublished data).

Mutated aequorins respond well to Ca^{2+} concentrations over the range (30–90 μM) which pertains within the secretory vesicle, as well as the rest of the secretory pathway (200–300 μM) (Montero et al., 1997; Pinton et al., 1998), without significant interference from the low pH environment. This feature of aequorin contrasts with GFP-based Ca^{2+} probes (Miyawaki et al., 1997; Baird et al., 1999; Emmanouilidou et al., 1999), whose fluorescence is strongly reduced at acidic pHs (Miesenbock et al., 1998; Fig. 2 E). Thus, aequorin may represent the most suitable molecularly targetable Ca^{2+} reporter presently available for the secretory vesicle interior.

Free Ca^{2+} concentration in the secretory vesicle lumen

Despite possessing a larger total Ca^{2+} content (Andersson et al., 1982; Hutton et al., 1983; Nicaise et al., 1992), secretory vesicles displayed a significantly lower free [Ca^{2+}] than the ER or Golgi apparatus. Our measured values for $[Ca^{2+}]_{SV}$ (~50 μM) correspond fairly well to measurements using other techniques in isolated chromaffin granules (Krieger-Brauer and Gratzl, 1982; 24 μM; null point titration), respiratory tract goblet cells (24 μM; calcium orange 5 N fluorescence; Nguyen et al., 1998) and platelet α-granules (12 μM; null point titration; Grinstein et al., 1983). Thus, free Ca^{2+} represents <0.05% of the total vesicular calcium content of β-cell secretory vesicles (assuming a total Ca^{2+} concentration of 50–100 mM; Hutton et al., 1983). Secretory vesicles appear to have the highest Ca^{2+}-buffering capacity of all subcellular organelles so far examined, with the percentage of free Ca^{2+} being much higher both in the cytosol (~2%) and in the ER (~10%; Pozzan et al., 1994). Importantly, resting $[Ca^{2+}]_{SV}$ was well below the K_M for Ca^{2+} of proinsulin-processing enzymes (Davidson et al., 1988).

The identity of the Ca^{2+} binding proteins (or other molecules) responsible for chelating free Ca^{2+} in these vesicles is unknown. Chromogranins (Yoo and Albanesi, 1990), or the mammalian homologue of *Tetrahymena thermophila* granule lattice protein 1 (Grlp1) (Chilcoat et al., 1996), are each strong possibilities. In addition, Ca^{2+} chelation by small molecules, such as ATP (Hutton et al., 1983), may also be involved. Finally, it is likely that in islet β-cells the insulin crystal itself also participates in chelating vesicular Ca^{2+} (Palmieri et al., 1988; see below).

Uptake of Ca^{2+} into secretory vesicles

The dense core secretory vesicle pool of islet β-cells has previously been considered relatively inert (Howell et al., 1975; Prentki et al., 1984). We provide evidence here that net uptake of Ca^{2+} into the dense core secretory vesicle population occurs during activated Ca^{2+} influx (Figs. 2 and 3), and in response to a receptor agonist (Fig. 5) or to nutrients (Fig. 8). However, and as discussed below (see also Fig. 9), these measurements do not exclude the possibility that discrete vesicle pools may experience different $[Ca^{2+}]_{SV}$ changes.

We considered the possibility that the increases in $[Ca^{2+}]_{SV}$ observed upon challenge of cells with agonists (Fig. 5) or nutrients (Fig. 8) may be due in part to the activation of exocytosis, and thus the exposure of aequorin within the vesicle matrix to the extracellular Ca^{2+} concentrations (1.5 mM). However, this phenomenon is likely to contribute negligibly to the observed signals, since only a tiny fraction of the total vesicle population (the "primed" pool) in β-cells (5–20/13,000 per min; Rorsman, 1997) undergoes fusion,

Published September 24, 2001

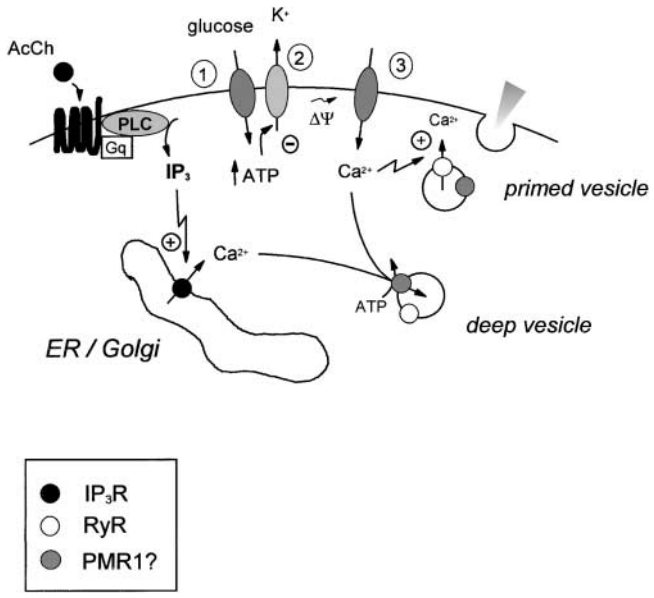

Figure 9. **Scheme: redistribution of organellar Ca^{2+} in secretory cells in response to G protein–coupled receptors (e.g., acetyl choline, AcCh) or glucose.** IP_3 generated in response to AcCh releases Ca^{2+} from the endoplasmic reticulum and Golgi apparatus, leading to an increase in cytosolic $[Ca^{2+}]$ and uptake of Ca^{2+} into dense core secretory vesicles distant from the plasma membrane (deep vesicles). Vesicular Ca^{2+} uptake is catalyzed by an undefined Ca^{2+}-ATPase, with properties similar to PMR1/ATP2C1 (see Discussion). Increases in blood glucose lead to (1) the uptake of the sugar via glucose transporters, (2) enhanced ATP synthesis and closure of ATP-sensitive K^+ channels, and (3) Ca^{2+} influx through L-type Ca^{2+} channels. The resultant increases in $[Ca^{2+}]_c$ are likely to promote net Ca^{2+} uptake (reflecting the balance of uptake versus release) into vesicles distant from the cell surface (deep vesicles). For those vesicles (<0.5% of total; Rorsman, 1997) located close to the plasma membrane and primed for exocytosis (primed vesicles), larger local $[Ca^{2+}]_c$ increases (e.g., at the mouth of activated plasma membrane Ca^{2+} channels; Neher, 1998) may activate vesicular RyRs and provoke net Ca^{2+} release.

even during the maximal stimulation of exocytosis. Consistent with this, we could detect no significant net movement of VAMP.GFP fluorescence to the plasma membrane after stimulation with DHPG (Fig. 5 D) or nutrients (Fig. 8 B).

Changes in intravesicular Ca^{2+} concentration detected with vesicle-targeted aequorin seem likely to result largely from the flux of Ca^{2+} ions across the vesicle membrane. However, two caveats are important: (a) Ca^{2+} release from/association with binding sites (or a "polyanionic matrix") (Nguyen et al., 1998) within the vesicle may also occur, especially if the intravesicular concentrations of other ions (e.g., K^+) change; (b) the number of Ca^{2+} ions that are transported is unknown, since this depends on the binding to intraorganellar sites. As discussed above, the present studies demonstrate that the ratio of free to bound Ca^{2+} within the secretory vesicles is much lower than that in the ER or Golgi lumen. This would appear at first to suggest that changes in intravesicular Ca^{2+} concentration must involve the flux of a very large number of Ca^{2+} ions. However, an alternative possibility is that there are two (or more) pools of bound Ca^{2+} in the secretory vesicle, one (the larger) comprising Ca^{2+} which is tightly bound (perhaps to a structural component such as the insulin crystal) and the other a more loosely bound and readily exchangeable pool. Depletion of this latter, "labile" pool, may thus lead to a substantial decrease in the free vesicular $[Ca^{2+}]$, while involving the release into the cytosol of relatively few Ca^{2+} ions.

The present data suggest that Ca^{2+} accumulation into vesicles is catalyzed at physiological $[Ca^{2+}]_c$ chiefly by a P-type Ca^{2+}-ATPase. Previous studies have indicated that transport of Ca^{2+} into the Golgi apparatus is mediated partly by a SERCA pump, and partly by another, unidentified thapsigargin-insensitive system (Pinton et al., 1998). This second ATP-dependent Ca^{2+} uptake system may be closely related to ATP2C1 (Hu et al., 2000), the mammalian homologue of the yeast Golgi Ca^{2+} transport ATPase, PMR1 (Sorin et al., 1997). Supporting this view, mRNA-encoding ATP2C1 is abundant in MIN6 cells, and polyclonal antibodies raised to ATP2C1 reveal a punctate pattern of intracellular staining (unpublished data). Intriguingly, although patients defective in the *ATP2C1* gene develop skin lesions ("Hailey-Hailey" disease; Hu et al., 2000), it is unclear whether these individuals also tend to suffer from neuroendocrine or other disorders (e.g., diabetes mellitus).

Secretory vesicles are an IP_3-insensitive, but caffeine/cADPr-sensitive Ca^{2+} store

The present results suggest that IP_3 is unlikely to stimulate the release of Ca^{2+} from dense core secretory vesicles directly (Fig. 5).

By contrast, we now show (Figs. 6 and 7) that functional RyR channels are present on the dense core vesicle membrane of MIN6 cells. Type II RyR mRNA is present in *ob/ob* mouse islets, mouse β-TC3 cells (Islam et al., 1998), and in rat islets (Holz et al., 1999). RyR II protein has been detected in INS1 β-cells (Gamberucci et al., 1999), and ryanodine binding sites revealed in human islets (Holz et al., 1999), mouse islets and MIN6 cells (Varadi and Rutter, 2001). Evidence for functional RyRs on the ER INS-1 β-cells (Maechler et al., 1999) has also recently been provided. The present data indicate that dense core vesicles may represent a large fraction (~30%) of the total RyR–accessible Ca^{2+} pool in MIN6 β-cells (Fig. 7 B). However, the proportion of the total vesicular Ca^{2+} pool which is mobilizable via RyR is small. Thus, the $[Ca^{2+}]_c$ increases observed when the total acidic Ca^{2+} pool was emptied with CPA, ionomycin, and monensin (Fig. 7 D) were much larger than those apparent when cells were treated with 4-CEP after CPA and ionomycin (Fig. 7 C).

Role of cADPr in β-cells

In the present studies, cADPr caused an apparent release of Ca^{2+} from both the ER and from the secretory vesicles in permeabilized MIN6 β-cells. Moreover, we have recently observed (Varadi and Rutter, 2001) that photolysis of caged cADPr increases $[Ca^{2+}]_c$ in MIN6 cells. These findings were surprising in light of earlier results using *ob/ob* mouse islets (Islam et al., 1993) or INS-1 β-cells (Rutter et al., 1994), where cADPr was ineffective in permeabilized cells. However, it should be noted that the present studies may provide greater sensitivity to small Ca^{2+} fluxes by measuring changes in $[Ca^{2+}]$ inside the secretory vesicle or ER.

Published September 24, 2001

Could changes in intracellular cADPr concentration play a role in the regulation of insulin secretion as proposed by Takasawa et al. (1993)? Supporting this view, mice homozygous for inactivation of the *CD38* (ADPribose cyclase) gene display impaired glucose tolerance (Kato et al., 1999). However, no change in the islet cADPr content was observed by others in response to acutely elevated glucose concentrations in vitro (Scruel et al., 1998), suggesting further studies are necessary.

Conclusions

Dense core secretory vesicles rapidly take up Ca^{2+} ions via an ATP-dependent non-SERCA Ca^{2+} pump (see Scheme, Fig. 9). Ca^{2+} accumulated into vesicles may later be released via RyRs once these vesicles reach a high local Ca^{2+} concentration beneath the plasma membrane (Neher, 1998) or elsewhere in the cell. This release may further contribute to the high local $[Ca^{2+}]_c$ in the vicinity of the submembrane vesicles (Emmanouilidou et al., 1999), and may be important to trigger exocytosis (Scheenen et al., 1998).

Materials and methods

Materials

Cell culture reagents were obtained from GIBCO BRL or Sigma-Aldrich and molecular biologicals from Roche Diagnostics. Fura-2 and cADPr were from Sigma-Aldrich and IP_3 was from Molecular Probes.

Construction of VAMP.Aq cDNA

VAMP2 cDNA was amplified by PCR using specific primers (forward: 5′-AAG CTT ACC ATG TCG GCT ACC GCT GCC ACC-3′; reverse: 5′-AAG CTT AGT GCT GAA GTA AAC GAT GAT-3′, HindIII sites are underlined). This fragment was then inserted upstream of the HindIII-EcoRI fragment encoding HA1-tagged D^{119}-A aequorin (Kendall et al., 1992) in plasmid pBS+. Chimeric VAMP.Aq cDNA was shuttled as a NotI-XhoI fragment into pcDNAI (Invitrogen; Fig. 1 A).

Construction of adenoviral VAMP.Aq and ER.Aq

ER.Aq (Montero et al., 1995) and VAMP.Aq cDNAs were transferred into plasmid pShuttleCMV (He et al., 1998) as Kpn1-Xho1 and Xba1-HindIII fragments, respectively. The resultant constructs were recombined with vector pAdEasy-1, and viral particles were generated as described (Ainscow and Rutter, 2001).

Cell culture, transient transfection, and adenoviral infection

MIN6 β-cells (Miyazaki et al., 1990; passages #20 and #30) were cultured in DME, with additions as given previously (Ainscow and Rutter, 2001). Cells cultured on 13 mm poly-L-lysine–coated coverslips were transfected with VAMP.Aq or ER.Aq plasmid DNA (1 μg) using Lipofectamine (Promega) in Optimem I serum-free medium (GIBCO BRL), or infected with adenoviruses as described (Ainscow and Rutter, 2001). The total quantity of reconstituted aequorin was higher in cells transfected with ER.Aq than VAMP.Aq cDNAs due to the inclusion in the former of intronic regulatory elements. Thus, typical integrated counts/culture (Fig. 2) after the expression of VAMP.Aq were 3×10^5 and 1.5×10^6 for conventional and adenoviral expression, respectively, and 2×10^6 and 2×10^7 for ER.Aq.

[Ca^{2+}] measurement with expressed aequorins

Cells were Ca^{2+} depleted by incubation with ionomycin (10 μM), the SERCA inhibitor CPA (10 μM; Mason et al., 1991; Pinton et al., 1998), and monensin (10 μM) in modified Krebs-Ringer bicarbonate buffer (KRB; 140 mM NaCl, 3.5 mM KCl, 0.5 mM NaH_2PO_4, 0.5 mM $MgSO_4$, 3 mM glucose, 10 mM Hepes, 2 mM $NaHCO_3$, pH 7.4) supplemented with 1 mM EGTA for 5 min at 4°C. Aequorin was reconstituted in 0.1 mM EGTA, 5 μM coelenterazine (cytosolic aequorin) or coelenterazine *n* (Shimomura et al., 1993; VAMP.Aq, ER.Aq) for 1–2 h at 4°C.

Intact cells were perifused (2 mL/min^{-1}) with KRB plus additions as stated (37°C) close to a photomultiplier tube (ThornEMI), and emitted light was collected (one data point) with a photon-counting board (ThornEMI; Cobbold and Rink, 1987). Where indicated, cells were permeabilized with digitonin (20 μM, 1 min at 22°C) and subsequently perifused in intracellular buffer (IB) (140 mM KCl, 10 mM NaCl, 1 mM KH_2PO_4, 5.5 mM glucose, 2 mM $MgSO_4$, 1 mM ATP, 2 mM Na^+ succinate, 20 mM Hepes, pH 7.05) at 37°C.

[Ca^{2+}] imaging with fura-2

Cells were loaded with 5 μM fura-2-AM (Sigma-Aldrich) for 40 min (37°C) in KRB plus 0.05% Pluronic F-127 (BASF). $[Ca^{2+}]_c$ was monitored in single cells at 37°C as described (Ainscow et al., 2000), using a Leica DM-IRBE inverted microscope (40× objective), and a Hamamatsu C4742-995 charge-coupled device camera driven by OpenLab (Improvision) software.

Imaging acridine orange fluorescence

Permeabilized cells were loaded with 3 μM acridine orange (Tsuboi et al., 2000) before imaging (37°C) on a Leica DM-IRBE™ inverted optics epiflurosecence microscope, at 493 ± 10 excitation, 530 nm emission (filters were from Chroma Techology).

Immunocytochemistry

48 h after transfection or infection, cells were fixed in 3.7% (vol/vol) paraformaldehyde and probed with antibodies essentially as described (Pouli et al., 1998a).

Immunoelectron microscopy

Gelatin-embedded, aldehyde-fixed cells were frozen in liquid nitrogen and ultrathin cryosections were obtained with a Reichert-Jung Ultracut E. Immunogold localization was performed as described (Confalonieri et al., 2000). Sections were immunostained either with rabbit anti-HA antibody (Sigma-Aldrich), or with a sheep anti-RyR antibody (Molecular Probes) followed by 10-nm protein A-gold. For double labeling, anti-HA–labeled sections were incubated with 1% glutaraldehyde in 0.1 M Na_2PO_4, pH 7.0, followed by incubation with a guinea pig antiinsulin antibody (Dako) and 15-nm protein A-gold. Sections were examined with a ZEISS EM 902 electron microscope. No labeling was detected in control sections (unpublished data).

Confocal imaging

Cells were imaged at 37°C on a Leica SP2 confocal spectrophotometer, (488 nm excitation) using a 100× oil immersion objective.

Other methods and statistics

Free [Ca^{2+}] and [Mg^{2+}] were calculated using "METLIG" (Rutter and Denton, 1988). Data are presented as the mean ± SEM for the number of observations given, and statistical significance calculated using Student's *t* test.

We thank Dr. Mark Jepson and Alan Leard (Bristol MRC Cell Imaging Facility) for their assistance with cell imaging, Dr. Nadia Todesco for help with the construction of VAMP.Aq cDNA, Maria Cristina Gagliani for help in electron microscopy, and Dr. Elek Molnar for the provision of mGluR5 cDNA and DHPG.

Supported by grants to G.A. Rutter from the Medical Research Council (UK), Human Frontiers Science Program, the Wellcome Trust, the Biotechnology and Biological Research Council, DiabetesUK, and the European Union; and to R. Rizzuto from Italian "Telethon" (Projects 850 and E0942), the Italian University and Health Ministries, the Italian Space Agency, The Italian National Research Council, The Armenise Harvard Foundation, and the Italian Association for Cancer Research.

Submitted: 30 March 2001
Revised: 23 July 2001
Accepted: 10 August 2001

References

Ainscow, E.K., and G.A. Rutter. 2001. Mitochondrial priming modifies Ca^{2+} oscillations and insulin secretion in pancreatic islets. *Biochem. J.* 353:175–180.

Ainscow, E.K., C. Zhao, and G.A. Rutter. 2000. Acute overexpression of lactate dehydrogenase-A perturbs β-cell mitochondrial metabolism and insulin secretion. *Diabetes*. 49:1149–1155.

Andersson, T., P.O. Berggren, E. Gylfe, and B. Hellman. 1982. Amounts and distribution of intracellular magnesium and calcium in pancreatic β-cells. *Acta.*

Physiol. Scand. 114:235–241.

Andrews, S.B., and T.S. Reese. 1986. Intracellular structure and elemental analysis in rapid-frozen neurons. *Ann. NY Acad. Sci.* 483:284–294.

Ashcroft, F.M., and S.J.M. Ashcroft. 1992. Mechanisms of insulin secretion. *In* Insulin, Molecular Biology to Pathology. F.M. Ashcroft and S.J.H. Ashcroft, editors. Oxford University Press, Oxford, NY. 97–150.

Baird, G.S., D.A. Zacharias, and R.Y. Tsien. 1999. Circular permutation and receptor insertion within green fluorescent proteins. *Proc. Natl. Acad. Sci. USA.* 96:11241–11246.

Berridge, M.J. 1993. Inositol trisphosphate and calcium signalling. *Nature.* 361: 315–325.

Blinks, J.R. 1989. Use of calcium-regulated photoproteins as intracellular Ca^{2+} indicators. *Methods Enzymol.* 172:164–203.

Blondel, O., M.M. Moody, A.M. Depaoli, A.H. Sharp, C.A. Ross, H. Swift, and G.I. Bell. 1994. Localization of inositol trisphosphate receptor subtype 3 to insulin and somatostatin secretory granules and regulation of expression in islets and insulinoma cells. *Proc. Natl. Acad. Sci. USA.* 91:7777–7781.

Brini, M., M. Murgia, L. Pasti, D. Picard, T. Pozzan, and R. Rizzuto. 1993. Nuclear Ca^{2+} concentration measured with specifically targeted recombinant aequorin. *EMBO J.* 12:4813–4819.

Bryan, J., and L. AguilarBryan. 1997. The ABCs of ATP-sensitive potassium channels: more pieces of the puzzle. *Curr. Opin. Cell Biol.* 9:553–559.

Carafoli, E. 1991. Calcium pump of the plasma membrane. *Physiol. Rev.* 71:129–153.

Chilcoat, N.D., S.M. Melia, A. Haddad, and A.P. Turkewitz. 1996. Granule lattice protein 1 (Grl1p), an acidic, calcium-binding protein in Tetrahymena thermophila dense-core secretory granules, influences granule size, shape, content organization, and release but not protein sorting or condensation. *J. Cell Biol.* 135:1775–1787.

Chini, E.N., and T.P. Dousa. 1996. Palmitoyl-CoA potentiates the Ca^{2+} release elicited by cyclic ADP-ribose. *Am. J. Physiol.* 270:C530–C537.

Cobbold, P.H., and T.J. Rink. 1987. Fluorescence and bioluminescence measurment of cytoplasmic free calcium. *Biochem. J.* 248:313–328.

Confalonieri, S., A.E. Salcini, C. Puri, C. Tacchetti, and P.P. Di Fiore. 2000. Tyrosine phosphorylation of Eps15 is required for ligand-regulated, but not constitutive, endocytosis. *J. Cell Biol.* 150:905–912.

Davidson, H.W., C.J. Rhodes, and J.C. Hutton. 1988. Intraorganellar calcium and pH control proinsulin cleavage in the pancreatic β cell via two distinct site-specific endopeptidases. *Nature.* 333:93–96.

Emmanouilidou, E., A. Teschemacher, A.E. Pouli, L.I. Nicholls, E.P. Seward, and G.A. Rutter. 1999. Imaging $[Ca^{2+}]$ changes at the secretory vesicle surface with a recombinant targeted cameleon. *Curr. Biol.* 9:918.

Galione, A. 1994. Cyclic ADP-ribose, the ADP-ribosyl cyclase pathway and calcium signalling. *Mol. Cell. Endocrinol.* 98:125–131.

Gamberucci, A., R. Fulceri, W. Pralong, G. Banhegyi, P. Marcolongo, S.L. Watkins, and A. Benedetti. 1999. Caffeine releases a glucose-primed endoplasmic reticulum Ca^{2+} pool in the insulin secreting cell line INS-1. *FEBS Lett.* 446:309–312.

Gerasimenko, O.V., J.V. Gerasimenko, P.V. Belan, and O.H. Petersen. 1996. Inositol trisphosphate and cyclic ADP-ribose-mediated release of Ca^{2+} from single isolated pancreatic zymogen granules. *Cell.* 84:473–480.

Gerasimenko, J.V., A.V. Tepikin, O.H. Petersen, and O.V. Gerasimenko. 1998. Calcium uptake via endocytosis with rapid release from acidifying endosomes. *Curr. Biol.* 8:1335–1338.

Goncalves, P.P., S.M. Meireles, C. Gravato, and M.G. Vale. 1998. Ca^{2+}-H^+ antiport activity in synaptic vesicles isolated from sheep brain cortex. *Neurosci. Lett.* 247:87–90.

Grapengiesser, E., E. Gylfe, and B. Hellman. 1988. Glucose-induced oscillations of cytoplasmic Ca^{2+} in the pancreatic β-cell. *Biochem. Biophys. Res. Commun.* 151:1299–1304.

Grinstein, S., W. Furuya, M.J. Vander, and R.G. Hancock. 1983. The total and free concentrations of Ca^{2+} and Mg^{2+} inside platelet secretory granules. Measurements employing a novel double null point technique. *J. Biol. Chem.* 258:14774–14777.

He, T.C., S. Zhou, L.T. da Costa, J. Yu, K.W. Kinzler, and B. Vogelstein. 1998. A simplified system for generating recombinant adenoviruses. *Proc. Natl. Acad. Sci. USA.* 95:2509–2514.

Hellman, B., J. Sehlin, and I.B. Taljedal. 1976. Calcium and secretion: distinction between two pools of glucose-sensitive calcium in pancreatic islets. *Science.* 194:1421–1423.

Holz, G.G., C.A. Leech, R.S. Heller, M. Castonguay, and J.F. Habener. 1999. cAMP-dependent mobilization of intracellular Ca^{2+} stores by activation of ryanodine receptors in pancreatic β-cells. A Ca^{2+} signaling system stimulated by the insulinotropic hormone glucagon-like peptide-1-(7-37). *J. Biol. Chem.* 274:14147–14156.

Howell, S.L., W. Montague, and M. Tyhurst. 1975. Calcium distribution in islets of Langerhans: a study of calcium concentrations and of calcium accumulation in B cell organelles. *J. Cell Sci.* 19:395–409.

Hu, Z., J.M. Bonifas, J. Beech, G. Bench, T. Shigihara, H. Ogawa, S. Ikeda, T. Mauro, and E.H. Epstein, Jr. 2000. Mutations in ATP2C1, encoding a calcium pump, cause Hailey-Hailey disease. *Nat. Genet.* 24:61–65.

Hutton, J.C., E.J. Penn, and M. Peshavaria. 1983. Low-molecular-weight constituents of isolated insulin-secretory vesicles. Bivalent cations, adenine nucleotides and inorganic phosphate. *Biochem. J.* 210:297–305.

Inouye, S., M. Noguchi, Y. Sakaki, Y. Takagi, T. Miyata, S. Iwanaga, T. Miyata, and F.I. Tsuji. 1985. Cloning and sequence analysis of cDNA for the luminescent protein aequorin. *Proc. Natl. Acad. Sci. USA.* 82:3154–3158.

Islam, M.S., O. Larsson, and P.O. Berggren. 1993. Cyclic ADP-ribose and pancreatic β cells. *Science.* 262:1499.

Islam, M.S., I. Leibiger, B. Leibiger, D. Rossi, V. Sorrentino, T.J. Ekstrom, H. Westerblad, F.H. Andrade, and P.O. Berggren. 1998. In situ activation of the type 2 ryanodine receptor in pancreatic β cells requires cAMP-dependent phosphorylation. *Proc. Natl. Acad. Sci. USA.* 95:6145–6150.

Kato, I., Y. Yamamoto, M. Fujimura, N. Noguchi, S. Takasawa, and H. Okamoto. 1999. CD38 disruption impairs glucose-induced increases in cyclic ADP-ribose, $[Ca^{2+}]$i, and insulin secretion. *J. Biol. Chem.* 274:1869–1872.

Kendall, J.M., G. SalaNewby, V. Ghalaut, R.L. Dormer, and A.K. Campbell. 1992. Engineering the Ca^{2+} activated photoprotein aequorin with reduced affinity for calcium. *Biochem. Biophys. Res. Commun.* 187:1091–1097.

Kennedy, H.J., A.E. Pouli, L.S. Jouaville, R. Rizzuto, and G.A. Rutter. 1999. Glucose-induced ATP microdomains in single islet β-cells. *J. Biol. Chem.* 274: 13281–13291.

Krieger-Brauer, H., and M. Gratzl. 1982. Uptake of Ca^{2+} by isolated secretory vesicles from adrenal medulla. *Biochim. Biophys. Acta.* 691:61–70.

Lai, F.A., H.P. Erickson, E. Rousseau, Q.Y. Liu, and G. Meissner. 1988. Purification and reconstitution of the calcium release channel from skeletal muscle. *Nature.* 331:315–319.

Maechler, P., E.D. Kennedy, E. Sebo, A. Valeva, T. Pozzan, and C.B. Wollheim. 1999. Secretagogues modulate the calcium concentration in the endoplasmic reticulum of insulin-secreting cells. Studies in aequorin-expressing intact and permeabilized INS-1 cells. *J. Biol. Chem.* 274:12583–12592.

Mason, M.J., C. Garcia-Rodriguez, and S. Grinstein. 1991. Coupling between intracellular Ca^{2+} stores and the Ca^{2+} permeability of the plasma membrane. Comparison of the effects of thapsigargin, 2,5-di-(tert-butyl)-1,4-hydroquinone, and cyclopiazonic acid in rat thymic lymphocytes. *J. Biol. Chem.* 266:20856–20862.

Miesenbock, G., D.A. De Angelis, and J.E. Rothman. 1998. Visualizing secretion and synaptic transmission with pH-sensitive green fluorescent proteins. *Nature.* 394:192–195.

Mikoshiba, K. 1997. The InsP3 receptor and intracellular Ca^{2+} signaling. *Curr. Opin. Neurobiol.* 7:339–345.

Miyawaki, A., J. Llopis, R. Heim, J.M. McCaffery, J.A. Adams, M. Ikura, and R.Y. Tsien. 1997. Fluorescent indicators for Ca^{2+} based on green fluorescent proteins and calmodulin. *Nature.* 388:882–887.

Miyazaki, J., K. Araki, E. Yamato, H. Ikegami, T. Asano, Y. Shibasaki, Y. Oka, and K. Yamamura. 1990. Establishment of a pancreatic β cell line that retains glucose inducible insulin secretion: special reference to expression of glucose transporter isoforms. *Endocrinology.* 127:126–132.

Moller, J.V., B. Juul, and M. le Maire. 1996. Structural organization, ion transport, and energy transduction of P-type ATPases. *Biochim. Biophys. Acta.* 1286:1–51.

Montero, M., M. Brini, R. Marsault, J. Alvarez, R. Sitia, T. Pozzan, and R. Rizzuto. 1995. Monitoring dynamic changes in free Ca^{2+} concentration in the endoplasmic reticulum of intact cells. *EMBO J.* 14:5467–5475.

Montero, M., J. Alvarez, W.J. Scheenen, R. Rizzuto, J. Meldolesi, and T. Pozzan. 1997. Ca^{2+} homeostasis in the endoplasmic reticulum: coexistence of high and low $[Ca^{2+}]$ subcompartments in intact HeLa cells. *J. Cell Biol.* 139:601–611.

Neher, E. 1998. Vesicle pools and Ca^{2+} microdomains: new tools for understanding their roles in neurotransmitter release. *Neuron.* 20:389–399.

Nguyen, T., W.C. Chin, and P. Verdugo. 1998. Role of Ca^{2+}/K^+ ion exchange in intracellular storage and release of Ca^{2+}. *Nature.* 395:908–912.

Nicaise, G., K. Maggio, S. Thirion, M. Horoyan, and E. Keicher. 1992. The calcium loading of secretory granules. A possible key event in stimulus-secre-

tion coupling. *Biol. Cell.* 75:89–99.

Orci, L., M. Ravazzola, M. Amherdt, O. Madsen, J.D. Vassalli, and A. Perrelet. 1985. Direct identification of prohormone conversion site in insulin-secreting cells. *Cell.* 42:671–681.

Palmieri, R., R.W. Lee, and M.F. Dunn. 1988. 1H Fourier transform NMR studies of insulin: coordination of Ca^{2+} to the Glu(B13) site drives hexamer assembly and induces a conformation change. *Biochemistry.* 27:3387–3397.

Parekh, A.B., and R. Penner. 1997. Store depletion and calcium influx. *Physiol. Rev.* 77:901–930.

Pezzati, R., M. Bossi, P. Podini, J. Meldolesi, and F. Grohovaz. 1997. High-resolution calcium mapping of the endoplasmic reticulum-Golgi-exocytic membrane system. Electron energy loss imaging analysis of quick frozen-freeze dried PC12 cells. *Mol. Biol. Cell.* 8:1501–1512.

Pinton, P., T. Pozzan, and R. Rizzuto. 1998. The Golgi apparatus is an inositol 1,4,5-trisphosphate-sensitive Ca^{2+} store, with functional properties distinct from those of the endoplasmic reticulum. *EMBO J.* 17:5298–5308.

Pouli, A.E., H.J. Kennedy, J.G. Schofield, and G.A. Rutter. 1998a. Insulin targeting to the regulated secretory pathway after fusion with green fluorescent protein and firefly luciferase. *Biochem. J.* 331:669–675.

Pouli, A.E., E. Emmanouilidou, C. Zhao, C. Wasmeier, J.C. Hutton, and G.A. Rutter. 1998b. Secretory-granule dynamics visualized in vivo with a phogrin green fluorescent protein chimaera. *Biochem. J.* 333:193–199.

Pozzan, T., R. Rizzuto, P. Volpe, and J. Meldolesi. 1994. Molecular and cellular physiology of intracellular calcium stores. *Physiol. Rev.* 74:595–636.

Prentki, M., D. Janjic, T.J. Biden, B. Blondel, and C.B. Wollheim. 1984. Regulation of Ca^{2+} transport by isolated organelles of a rat insulinoma. Studies with endoplasmic reticulum and secretory granules. *J. Biol. Chem.* 259: 10118–10123.

Ravazzola, M., P.A. Halban, and L. Orci. 1996. Inositol 1,4,5-trisphosphate receptor subtype 3 in pancreatic islet cell secretory granules revisited. *Proc. Natl. Acad. Sci. USA.* 93:2745–2748.

Reetz, A., M. Solimena, M. Matteoli, F. Folli, K. Takei, and P. De Camilli. 1991. GABA and pancreatic B-cells: colocalization of glutamic acid decarboxylase (GAD) and GABA with synaptic-like microvesicles suggests their role in GABA storage and secretion. *EMBO J.* 10:1275–1284.

Rizzuto, R., M. Brini, M. Murgia, and T. Pozzan. 1993. Microdomains with high Ca^{2+} close to IP3-sensitive channels that are sensed by neighbouring mitochondria. *Science.* 262:744–747.

Rizzuto, R., M. Brini, C. Bastianutto, R. Marsault, and T. Pozzan. 1995. Photoprotein-mediated measurement of calcium ion concentration in mitochondria of living cells. *Methods Enzymol.* 260:417–428.

Rorsman, P. 1997. The pancreatic β-cell as a fuel sensor: an electrophysiologist's viewpoint. *Diabetologia.* 40:487–495.

Rutter, G.A., and R.M. Denton. 1988. Regulation of NAD^+-linked isocitrate dehydrogenase and 2-oxoglutarate dehydrogenase by Ca^{2+} ions within toluene-permeabilized rat heart mitochondria. Interactions with regulation by adenine nucleotides and $NADH/NAD^+$ ratios. *Biochem. J.* 252:181–189 (erratum published 253:935).

Rutter, G.A., J.-M. Theler, M. Murghia, C.B. Wollheim, T. Pozzan, and R. Rizzuto. 1993. Stimulated Ca^{2+} influx raises mitochondrial free Ca^{2+} to supramicromolar levels in a pancreatic β-cell line: possible role in glucose and agonist-induced insulin secretion. *J. Biol. Chem.* 268:22385–22390.

Rutter, G.A., J.-M. Theler, G. Li, and C.B. Wollheim. 1994. Ca^{2+} stores in insulin-secreting cells: lack of effect of cADP ribose. *Cell Calcium.* 16:71–80.

Rutter, G.A., C. Fasolato, and R. Rizzuto. 1998. Calcium and organelles: a two-sided story. *Biochem Biophys. Res. Commun.* 253:549–557.

Safayhi, H., H. Haase, U. Kramer, A. Bihlmayer, M. Roenfeldt, H.P. Ammon, M. Froschmayr, T.N. Cassidy, I. Morano, M.K. Ahlijanian, and J. Striessnig. 1997. L-type calcium channels in insulin-secreting cells: biochemical characterization and phosphorylation in RINm5F cells. *Mol. Endocrinol.* 11:619–629.

Scheenen, W.M., C.B. Wollheim, T. Pozzan, and C. Fasolato. 1998. Ca^{2+} depletion from granules inhibits exocytosis. A study with insulin-secreting cells. *J. Biol. Chem.* 273:19002–19008.

Scruel, O., T. Wada, K. Kontani, A. Sener, T. Katada, and W.J. Malaisse. 1998. Effects of D-glucose and starvation upon the cyclic ADP-ribose content of rat pancreatic islets. *Biochem. Mol. Biol. Int.* 45:783–790.

Shimomura, O., B. Musicki, Y. Kishi, and S. Inouye. 1993. Light-emitting properties of recombinant semi-synthetic aequorins and recombinant fluoresceinconjugated aequorin for measuring cellular calcium. *Cell Calcium.* 14:373–378.

Sorin, A., G. Rosas, and R. Rao. 1997. PMR1, a Ca^{2+}-ATPase in yeast Golgi, has properties distinct from sarco/endoplasmic reticulum and plasma membrane calcium pumps. *J. Biol. Chem.* 272:9895–9901.

Streb, H., E. Bayerdorffer, W. Haase, R.F. Irvine, and I. Schulz. 1984. Effect of inositol-1,4,5-trisphosphate on isolated subcellular fractions of rat pancreas. *J. Membr. Biol.* 81:241–253.

Sudhof, T.C., M. Baumert, M.S. Perin, and R. Jahn. 1989. A synaptic vesicle membrane protein is conserved from mammals to *Drosophila*. *Neuron.* 2:1475–1481.

Takasawa, S., K. Nata, H. Yonekura, and H. Okamoto. 1993. Cyclic ADP-ribose in insulin secretion from pancreatic B-cells. *Science.* 259:370–373.

Takeshima, H., S. Nishimura, T. Matsumoto, H. Ishida, K. Kangawa, N. Minamino, H. Matsuo, M. Ueda, M. Hanaoka, T. Hirose, et al. 1989. Primary structure and expression from complementary DNA of skeletal muscle ryanodine receptor. *Nature.* 339:439–445.

Thastrup, O. 1990. Role of Ca^{2+}-ATPases in regulation of cellular Ca^{2+} signalling, as studied with selective microsomal Ca^{2+}-ATPase inhibitor, thapsigargin. *Agents Actions.* 29:8–15.

Thirion, S., J.D. Troadec, N.B. Pivovarova, S. Pagnotta, S.B. Andrews, R.D. Leapman, and G. Nicaise. 1999. Stimulus-secretion coupling in neurohypophysial nerve endings: a role for intravesicular sodium? *Proc. Natl. Acad. Sci. USA.* 96:3206–3210.

Thomas, L.S., D.E. Jane, R. Harris, and M.J. Croucher. 2000. Metabotropic glutamate autoreceptors of the mGlu(5) subtype positively modulate neuronal glutamate release in the rat forebrain in vitro. *Neuropharmacology.* 39: 1554–1566.

Troadec, J.D., S. Thirion, J.P. Laugier, and G. Nicaise. 1998. Calcium-induced calcium increase in secretory vesicles of permeabilized rat neurohypophysial nerve terminals. *Biol. Cell.* 90:339–347.

Tsuboi, T., C. Zhao, S. Terakawa, and G.A. Rutter. 2000. Simultaneous evanescent wave imaging of insulin vesicle membrane and cargo during a single exocytotic event. *Curr. Biol.* 10:1307–1310.

Varadi, A., and G.A. Rutter. 2001. Dynamic imaging of endoplasmic reticulum [Ca^{2+}] in MIN6 cells using recombinant cameleons: roles of SERCA2 and ryanodine receptors. *Diabetes*. In press.

Yoo, S.H. 2000. Coupling of the IP_3 receptor/Ca^{2+} channel with Ca^{2+} storage proteins chromogranins A and B in secretory granules. *Trends Neurosci.* 23:424–428.

Yoo, S.H., and J.P. Albanesi. 1990. Inositol 1,4,5-trisphosphate-triggered Ca^{2+} release from bovine adrenal medullary secretory vesicles. *J. Biol. Chem.* 265: 13446–13448.

Yule, D.I., S.A. Ernst, H. Ohnishi, and R.J.H. Wojcikiewicz. 1997. Evidence that zymogen granules are not a physiologically relevant calcium pool. Defining the distribution of inositol 1,4,5-trisphosphate receptors in pancreatic acinar cells. *J. Biol. Chem.* 272:9093–9098.

Zorzato, F., E. Scutari, V. Tegazzin, E. Clementi, and S. Treves. 1993. Chlorocresol: an activator of ryanodine receptor-mediated Ca^{2+} release. *Mol. Pharmacol.* 44:1192–1201.